Supplement of Earth Surf. Dynam., 13, 1229–1248, 2025 https://doi.org/10.5194/esurf-13-1229-2025-supplement © Author(s) 2025. CC BY 4.0 License.





Supplement of

Improving a multi-grain-size total sediment load model through a new standardized reference shear stress for incipient motion and an adjusted saltation height description

Marine Le Minor et al.

Correspondence to: Marine Le Minor (marine.le-minor@univ-rennes.fr)

The copyright of individual parts of the supplement might differ from the article licence.

S.1 The erosion-deposition model of Le Minor et al. (2022)

S.1.1 Mass balance equation

Sediment transport is the consequence of exchanges between the water column that carries mobile grains and the sediment bed that consists of immobile grains. In the erosion-deposition model, deposition and erosion are two explicit fluxes, and thus, the mass balance equation of the transported sediment writes:

$$\frac{\partial \left(\overline{C}_{s,i}h\right)}{\partial t} + \operatorname{div}\left(q_{s,i}\right) = \dot{e}_i - \dot{d}_i$$

where $\overline{C_{s,i}}$ [-] is the depth-averaged sediment concentration, \dot{d}_i [m s⁻¹] is the deposition rate, \dot{e}_i [m s⁻¹] is the entrainment rate, h [m] is the water depth, $q_{s,i}$ [m² s⁻¹] is the sediment load per unit width and t [s] is the time.

S.1.2 Deposition rate

Based on formalism introduced by Kooi and Beaumont (1994) and further developed by Davy and Lague (2009), we assume that the deposition rate writes:

$$\dot{d}_i = \frac{q_{s,i}}{\xi_i}$$
 where ξ_i [m] is the sediment transport length.

S.1.3 Transport length

According to Auel et al. (2017), the velocity of grains in saltation $v_{salt,i}$ [m s⁻¹] writes as: $v_{salt,i} = \{ 1.46 \sqrt{R_i g d_i} T_i^{*0.5} \text{ if } T_i^* > 0 \\ 0 \text{ otherwise} \}$

$$v_{salt,i} = \begin{cases} 1.46 \sqrt{R_i g d_i} T_i^{*0.5} & \text{if } T_i^* > 0 \\ 0 & \text{otherwise} \end{cases}$$

In Le Minor et al., (2022), it was assumed that saltation velocities do not exceed the average water velocity $V_{laver,i}$ [m s⁻¹] over the characteristic transport height. In the water column, the flow velocity may be described by a logarithmic profile with velocities decreasing towards zero at the bed roughness height. Thus, this average velocity is calculated as:

$$v_{layer,i} = \left\{ \min \left(\frac{u_*}{\kappa} \left(\ln \left(\frac{h_{s,i}}{z_0} \right) - 1 + \frac{z_0}{h_{s,i}} \right), \overline{u} \right) \text{ if } T_i^* > 0 \right\}$$

where κ [-] is the von Kármán constant, \bar{u} [m s⁻¹] is the depth-averaged water velocity and u_* [m s⁻¹] is the shear velocity.

transport velocity $\overline{V_{s,i}}$ of transported grains writes: $\overline{v_{s,i}} = \begin{cases} \min(v_{salt,i}, v_{layer,i}) \text{ if } P_i \ge 2.5 \\ v_{layer,i} \text{ if } P_i < 2.5 \end{cases}$

where $P_i = \frac{w_{s,i}}{\kappa u_s}$ [-] is the Rouse number (Rouse, 1937) and $w_{s,i}$ [m s⁻¹] is the terminal sediment settling velocity.

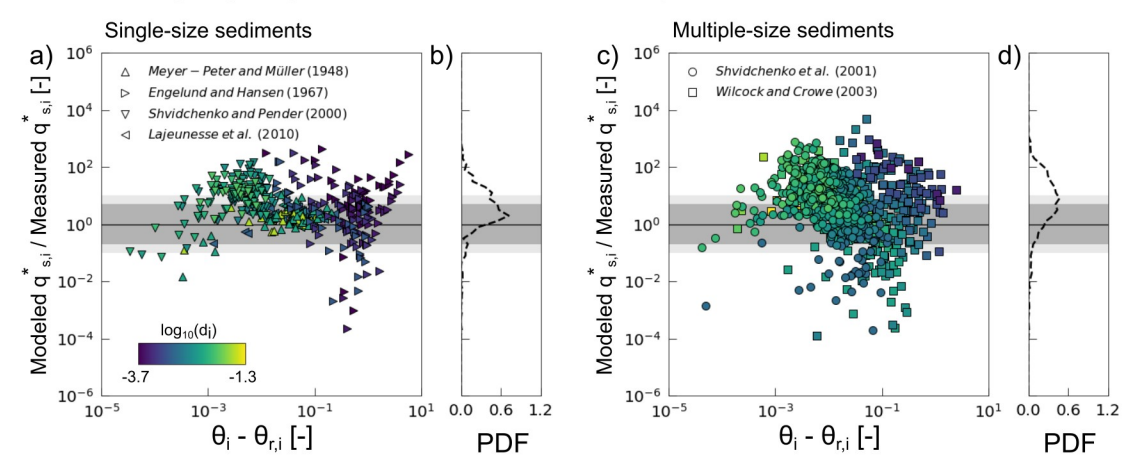
S.2 Summary of experimental conditions for each dataset

Table S1: Range of parameters for each dataset.

	Referenc e	Grain size [mm]	Density [kgm-3]	Final sand fraction	Slope [-]	Water depth [m]	Depth- averaged velocity [ms-1]	Shields stress corrected from wall effects [Pa]	Bedform s
Single grain size	Meyer- Peter and Müller (1948)	2 sizes 5.21 to 21.65	1250 to 4220	-	1.38e-3 to 22.7e- 3	0.008 to 1.092	0.239 to 2.880	0.048 to 0.0252	No
	Engelund and Hansen (1967)	5 sizes 0.19 to 0.93	2650	-	0.16e-3 to 12.8e-3	0.058 to 0.344	0.212 to 1.897	0.050 to 5.836	Yes
	Shvidche nko and Pender (2000)	8 sizes 1.5 to 12.0	2600 to 2650	-	1.9e-3 to 28.7e-3	0.014 to 0.136	0.065 to 1.074	0.025 to 0.083	Yes
	Lajeunes se et al. (2010)	3 sizes 1.15 to 5.5	2650 to 2660	-	0.16e-3 to 12.8e-3	0.005 to 0.016	0.266 to 0.830	0.008 to 0.257	No
Multiple grain sizes	Shvidche nko et al. (2001)	8 classes 1 to 14	2600 to 2650 (avg.: 2625)	0 to 37%	4.1e-3 to 14.1e-3	0.032 to 0.128	0.278 to 0.915	0.011 to 0.375	Yes
	Wilcock and Crowe (2003)	14 classes 0.1 to 64	2550 to 2710 (avg.: 2610)	0 to 60%	0.6e-3 to 20.4e-3	0.088 to 0.120	0.261 to 1.231	0.0006 to 4.131	No

S.3 Simplified transport velocity

Le Minor et al. (2022) - Original formulation of transport velocity



Le Minor et al. (2022) - Simplified formulation of transport velocity (Equation 13)

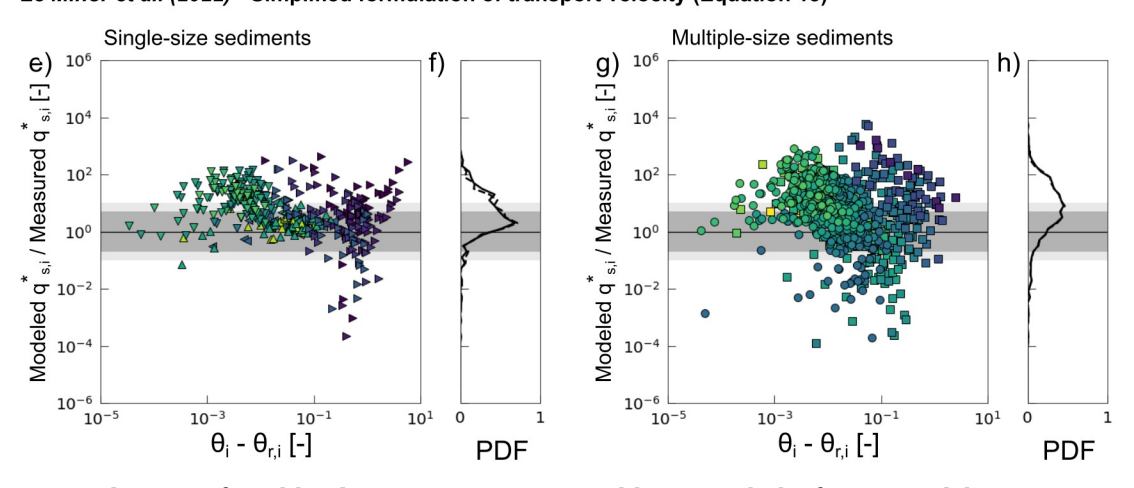


Figure S1: Predictions of total load transport rates at equilibrium with the former model parameterization of Le Minor et al. (2022) with and without the simplified version of LM2022's transport velocity. The ratio of model predictions to flume observations is plotted against the dimensionless excess of shear stress (Shields stress) along with the probability density function (PDF) of the residuals for single- (a-b, e-f) and multiple-size sediments (c-d, g-h). The dark and light gray areas correspond to measured values that are predicted within a factor of 5 and 10, respectively. For the PDF, the dashed and solid lines correspond to predictions in the reference case without and with the simplified version of LM2022's transport velocity.

S.4 Correlation of entrainment coefficient with key parameters

Table S2: Calibration of entrainment factor and transport rate predictions for both single- and multiple-size sediments considering single hypotheses at once. Percentage of predictions are indicated for multiple-size data where the bed surface is fully mobile and partially mobile. P-values are added in brackets. Simplified velocity used in all cases. Calibration carried out on single-size data and multiple-size data where the surface is fully mobile.

Table S3: Calibration of entrainment factor and transport rate predictions for both single- and multiple-size sediments considering combinations of hypotheses at once. Percentage of predictions are indicated for multiple-size data where the bed surface is fully mobile and partially mobile. P-values are added in brackets. Simplified velocity, standardized reference shear stress and adjusted transport length used in all cases. Calibration carried out on single-size data and multiple-size data where the surface is fully mobile.

S2	Calibrated entrainment factor α	Single-size sediments		Multiple-size sediments – All		Multiple-size sediments – Fully mobile only		Multiple-size sediments – Partially mobile only	
Adjustments		Factor 5	Factor 10	Factor 5	Factor 10	Factor 5	Factor 10	Factor 5	Factor 10
Ref. Le Minor et al. (2022)	$\alpha = \frac{\pi}{6} 37.64 = 19.71$	53%	65%	36%	51%	40%	57%	29%	42%
	$\alpha = \frac{\pi}{6} 37.64 = 19.71$	59%	80%	39%	55%	42%	61%	36%	51%
shear stress for incipient motion	$\alpha = 4.61$	81%	89%	54%	73%	62%	81%	46%	65%
Transport height	α = 2.51	79%	92%	62%	81%	68%	83%	57%	79%
Froude effect	$\alpha = 6.09 F_r^{0.33} (p=0.025, R^2=0.01)$	81%	89%	54%	71%	62%	78%	47%	65%
Relative roughness	$\alpha = 2.60 \left(\frac{d_i}{k_s}\right)^{-0.43} (p=0.000, R^2=0.07)$	79%	87%	53%	70%	63%	79%	45%	63%
	$\alpha = 3.16 \left(\frac{h}{z_0}\right)^{0.12} (p=0.040, R^2=0.01)$	82%	89%	53%	71%	61%	79%	46%	64%
	$\alpha = 2.60 \left(\frac{d_i}{k_s}\right)^{-0.43} (p=0.000, R^2=0.07)$ $\alpha = 3.16 \left(\frac{h}{z_0}\right)^{0.12} (p=0.040, R^2=0.01)$ $\alpha = 2.36 \left(\frac{h}{d_i}\right)^{0.26} (p=0.000, R^2=0.05)$	79%	87%	55%	72%	63%	81%	47%	65%
Particle Reynolds	$\alpha = 15.50 \mathrm{Re}_{p,i}^{-0.19} (p = 0.000, R^2 = 0.03)$	80%	90%	53%	71%	61%	79%	46%	64%
Mobile fraction	$\alpha = 7.15 F_{mobile}^{4.48} (p=0.000, R^2=0.09)$	-	-	-	-	-	-	52%	67%

S3	Calibrated entrainment factor α	Single-size sediments		Multiple-size sediments - All		Multiple-size sediments – Fully mobile only		Multiple-size sediments – Partially mobile only	
Adjustments		Factor 5	Factor 10	Factor 5	Factor 10	Factor 5	Factor 10	Factor 5	Factor 10
Froude effect	$\alpha = 2.96 F_r^{0.96} (p=0.000, R^2=0.08)$	80%	93%	64%	83%	69%	84%	60%	81%
Relative roughness	$\alpha = 2.45 \left(\frac{d_i}{k_s}\right)^{0.02} (p=0.702, R^2=0.00)$	78%	92%	62%	80%	68%	84%	57%	78%
	$\alpha = 2.45 \left(\frac{d_i}{k_s}\right)^{0.02} (p=0.702, R^2=0.00)$ $\alpha = 1.55 \left(\frac{h}{z_0}\right)^{0.09} (p=0.057, R^2=0.00)$ $\alpha = 2.13 \left(\frac{h}{d_i}\right)^{0.03} (p=0.294, R^2=0.00)$	79%	92%	62%	81%	68%	85%	57%	77%
	$\alpha = 2.13 \left(\frac{h}{d_i}\right)^{0.03} (p=0.294, R^2=0.00)$	78%	92%	63%	81%	68%	85%	58%	78%
Particle Reynolds	$\alpha = 2.20 \operatorname{Re}_{p,i}^{0.01} (p = 0.661, R^2 = 0.00)$	78%	92%	63%	81%	68%	84%	58%	78%
Mobile fraction	$\alpha = 2.51 F_{mobile}^{2.24}$ ($p = 0.000$, $R^2 = 0.07$) (forced to fit single-size data)	-	-	-	-	-	-	59%	80%
Froude effect +Relative	$\alpha = 2.26 F_r^{1.15} \left(\frac{d_i}{k_s} \right)^{-0.18}$	81%	95%	66%	84%	69%	86%	64%	83%
roughness	$(p=0.000, p=0.000, R^2=0.10)$ $\alpha = 0.78 F_r^{1.25} \left(\frac{h}{z_0}\right)^{0.28}$	80%	92%	65%	84%	71%	87%	60%	81%
	$(p=0.000, p=0.000, R^2=0.12)$ $\alpha = 1.37 F_r^{1.55} \left(\frac{h}{d_i}\right)^{0.27}$	84%	94%	68%	86%	73%	88%	65%	84%
Froude effect +Particle Reynolds	$(p=0.000, p=0.000, R^2=0.14)$ $\alpha = 7.02 F_r^{1.21} Re_{p,i}^{-0.15}$ $(p=0.000, p=0.000, R^2=0.10)$	81%	94%	65%	84%	70%	85%	62%	82%

Reynolds	$\alpha = 2.28 \left(\frac{d_i}{k_s}\right)^{0.01} \operatorname{Re}_{p,i}^{0.01}$ $(p = 0.840, p = 0.769, R^2 = 0.00)$ $\alpha = 0.67 \left(\frac{h}{z_0}\right)^{0.16} \operatorname{Re}_{p,i}^{0.09}$	78% 78%	92%	62% 63%	81%	68%	84%	57% 57%	78%
	$(p=0.005, p=0.037, R^{2}=0.01)$ $\alpha = 1.04 \left(\frac{h}{d_{i}}\right)^{0.10} \operatorname{Re}_{p,i}^{0.09}$ $(p=0.037, p=0.063, R^{2}=0.01)$	77%	91%	63%	82%	68%	85%	59%	79%
Froude effect	$\alpha = 4.86 F_r^{1.30} Re_{p,i}^{-0.12} \left(\frac{d_i}{k_s}\right)^{-0.13}$	83%	95%	67%	84%	70%	86%	64%	83%
roughness	$ \left \begin{array}{l} (p=0.000, \ p=0.002, \ p=0.013, \ R^2=0.11) \\ \alpha=1.21 F_r^{1.30} \operatorname{Re}_{p,i}^{-0.05} \left(\frac{h}{z_0}\right)^{0.25} \end{array} \right $	81%	93%	65%	84%	71%	87%	60%	81%
	$(p=0.000, p=0.249, p=0.000, R^2=0.12)$ $\alpha = 0.95 F_r^{1.53} \text{Re}_{p,i}^{0.05} \left(\frac{h}{d_i}\right)^{0.31}$	83%	94%	68%	85%	72%	87%	65%	84%
	$(p=0.000, p=0.301, p=0.000, R^2=0.15)$								